CHAPTER 6

TIME-AVERAGED WAVE FIELD EVOLUTION IN COASTAL ZONE

Jianlu Xu[1] and Rodney J. Sobey[2]

1. Introduction

Flow circulation and the field variation of wave height and setup are important data in coastal engineering practice. This paper presents a wave-averaged model for simulating wave transformation and associated mean flow circulation in coastal regions. It is intended for applications where interest centers on the evolution of wave-averaged parameters such as wave height, setup and wave-induced current, and where the resolution of wave phase is unnecessary.

2. Governing Equations

An analysis technique used in turbulent shear flow is adapted to develop the governing equations for wave height, wave setup and mean flow. Variables are decomposed into a slowly varying mean flow and a fluctuating residual which includes both wave and turbulent components. For example, a general velocity vector is decomposed into a wave-averaged velocity vector $(\overline{u}, \overline{v}, \overline{w})$ and a fluctuating velocity vector $(\tilde{u}, \tilde{v}, \tilde{w})$.

Subsequently the conservation equations of mass, momentum and energy are averaged over a wave period and integrated over water depth. The time-averaging introduces apparent stress- or Reynolds stress-style terms corresponding to the time scale of the wave period. The wave-averaged and depth-integrated continuity equation reads (Sobey & Thieke 1988).

$$\frac{\partial \overline{\eta}}{\partial t} + \frac{\partial}{\partial x}\int_{-h}^{\eta_c} \overline{u}dz + \frac{\partial}{\partial y}\int_{-h}^{\eta_c} \overline{v}dz = 0 \tag{1}$$

where x, y and z denote the Cartesian coordinates with z directed upward, t denotes the time, $\overline{\eta}$ is the local wave setup, η_c is the local wave crest elevation, and h is the local water depth from a datum plane in the global SWL. Equation (1) is identical to the long wave continuity equation.

The depth-integrated and wave-averaged x- and y-momentum equations are

---

1. Hydraulic Engineer, Bechtel Environmental Inc. San Francisco, CA 94119, USA
2. Professor, Department of Civil and Environmental Engineering, University of California at Berkeley, CA 94720, USA.

$$\frac{\partial}{\partial t}\int_{-h}^{\eta_c}\bar{u}dz+\frac{\partial}{\partial x}\int_{-h}^{\eta_c}\overline{u^2}dz+\frac{\partial}{\partial y}\int_{-h}^{\eta_c}\overline{uv}dz= -g(h+\bar{\eta})\frac{\partial\bar{\eta}}{\partial x}+\frac{1}{\rho}\left[\frac{\partial}{\partial x}\int_{-h}^{\eta_c}s_{xx}dz+\frac{\partial}{\partial y}\int_{-h}^{\eta_c}s_{xy}dz-\tau_{bx}\right] \tag{2}$$

$$\frac{\partial}{\partial t}\int_{-h}^{\eta_c}\bar{v}dz+\frac{\partial}{\partial x}\int_{-h}^{\eta_c}\overline{uv}dz+\frac{\partial}{\partial y}\int_{-h}^{\eta_c}\overline{v^2}dz= -g(h+\bar{\eta})\frac{\partial\bar{\eta}}{\partial y}+\frac{1}{\rho}\left[\frac{\partial}{\partial x}\int_{-h}^{\eta_c}s_{xy}dz+\frac{\partial}{\partial y}\int_{-h}^{\eta_c}s_{yy}dz-\tau_{by}\right] \tag{3}$$

where s_{xx}, s_{xy}, s_{yy} are wave apparent stresses, and τ_{bx} and τ_{by} are the bottom shear stress components in the x and y direction, respectively. The wave energy equation is written as

$$\frac{1}{2}\frac{\partial}{\partial t}\left[\int_{-h}^{\eta_c}(\overline{\tilde{u}^2}+\overline{\tilde{v}^2}+\overline{\tilde{w}^2})dz+g\overline{\tilde{\eta}^2}\right]+\frac{\partial}{\partial x}\int_{-h}^{\eta_c}\left[\frac{\overline{\tilde{p}_d\tilde{u}}}{\rho}+\frac{1}{2}(\overline{\tilde{u}^3}+\overline{\tilde{u}\tilde{v}^2}+\overline{\tilde{u}\tilde{w}^2})\right]dz$$
$$-\frac{\partial}{\partial y}\int_{-h}^{\eta_c}\left(\frac{\overline{\tilde{p}_d\tilde{v}}}{\rho}+\frac{(\overline{\tilde{v}\tilde{u}^2}+\overline{\tilde{v}^3}+\overline{\tilde{v}\tilde{w}^2})}{2}\right)dz=-\frac{\partial}{\partial x}\int_{-h}^{\eta_c}\frac{\bar{u}}{2}(\overline{\tilde{u}^2}+\overline{\tilde{v}^2}+\overline{\tilde{w}^2})dz-\frac{\partial\bar{u}}{\partial x}\int_{-h}^{\eta_c}\overline{\tilde{u}^2}dz \tag{4}$$
$$-\left(\frac{\partial\bar{v}}{\partial x}+\frac{\partial\bar{u}}{\partial y}\right)\int_{-h}^{\eta_c}\overline{\tilde{u}\tilde{v}}dz-\frac{\partial}{\partial y}\int_{-h}^{\eta_c}\frac{\bar{v}(\overline{\tilde{u}^2}+\overline{\tilde{v}^2}+\overline{\tilde{w}^2})}{2}dz-\frac{\partial\bar{v}}{\partial y}\int_{-h}^{\eta_c}\overline{\tilde{v}^2}dz-D_{bf}-D_{wb}$$

where D_{bf} and D_{wb} are energy dissipation due to bottom friction and wave breaking, respectively.

3. Closure Solution Surfaces

Equations (1)-(4) contain wave setup, mean flow velocity and wave apparent stresses, among other unknowns. The number of the unknowns far exceeds the number of governing equations. This is the apparent stress closure problem familiar in turbulence. As our closure hypothesis, the Reynolds stress-style terms are established as a function of wave height, wave period and water depth from Fourier approximation wave theory. For simplicity, the closure variables are defined in the propagation direction of plane waves. In addition, a two-layer flow structure is assumed with the kinematics above wave trough(surface layer) being dominated by wave motion and the mean flow current being confined below the wave trough(bottom layer). The closure parameters for the local layer-averaged wave apparent stresses are, e.g., defined as

$$S_s=\frac{1}{H}\int_{\eta_{tr}}^{\eta_c}[-\Delta p+\rho(\overline{\tilde{w}^2}-\overline{\tilde{u}^2})]dz \qquad \text{for the surface layer} \tag{5}$$

$$S_b=\frac{1}{h-\eta_{tr}}\int_{-h}^{\eta_{tr}}\rho(\overline{\tilde{w}^2}-\overline{\tilde{u}^2})dz \qquad \text{for the bottom layer} \tag{6}$$

where η_{tr} is the local wave trough elevation, and Δp is the local pressure residual due to the partial submergence of a point above the wave trough during a wave period. Sixteen closure variables(η_{tr}, $\hat{U}_s$, U_{rms}, $\hat{U}_s^2$, $\overline{U_b^3}$, S_s, S_b, N_s, N_b, W_s, W_b, $\overline{\eta^2}$, F_s, F_b, K_s and Ep) are similarly established and these closure variables are normalized by angular wave frequency ω and the acceleration due to gravity, g. For example, S_s and S_b are normalized by $\rho\cdot\omega^2/g^2$. Following the above procedure, closure solution surfaces are established with water depth ranging from deep to shallow and wave height upto the breaking limit.

Upon substituting the closure parameters into Equations (1) to (4), a closed system for the wave height, H, wave setup, $\overline{\eta}$, and mean flow velocity, U_b and V_b, is developed. The integral, dimensionless continuity equation reads

$$\frac{\partial\overline{\eta}}{\partial t}+\frac{\partial}{\partial x}[(H\,U_s\cos\phi)+(h+\overline{\eta}+\eta_{tr})U_b]+\frac{\partial}{\partial y}[(H\,U_s\sin\phi+(h+\overline{\eta}+\eta_{tr})V_b]=0 \quad (7)$$

The integral x- and y-momentum equations are

$$\begin{aligned}&\frac{\partial}{\partial t}[HU_s\cos\phi+(h+\overline{\eta}+\eta_{tr})U_b]+\frac{\partial}{\partial x}[H\,U_s^2\cos^2\phi+(h+\overline{\eta}+\eta_{tr})U_b^2+(h+\frac{\overline{\eta}}{2})\overline{\eta}]\\&+\frac{\partial}{\partial y}[H\,U_s^2\frac{\sin 2\phi}{2}+(h+\overline{\eta}+\eta_{tr})U_b\,V_b]=\_\overline{\eta}\frac{\partial h}{\partial x}+\frac{\partial}{\partial x}[H(S_s+\sin^2\phi\,N_s)\\&+(h+\overline{\eta}+\eta_{tr})(S_b+\sin^2\phi\,N_b)]-\frac{\partial}{\partial y}[\frac{\sin 2\phi}{2}(H\,N_s+(h+\overline{\eta}+\eta_{tr})N_b)]-\frac{\tau_{bx}}{\rho}\end{aligned} \quad (8)$$

$$\begin{aligned}&\frac{\partial}{\partial t}[H\,U_s\sin\phi+(h+\overline{\eta}+\eta_{tr})V_b]+\frac{\partial}{\partial x}[H\,U_s^2\cos^2\phi+(h+\overline{\eta}+\eta_{tr})U_b\,V_b]\\&+\frac{\partial}{\partial y}[H\,U_s^2\sin^2\phi+(h+\overline{\eta}+\eta_{tr})V_b^2+(h+\frac{\overline{\eta}}{2})\overline{\eta}]=-\overline{\eta}\frac{\partial h}{\partial y}-\frac{\partial}{\partial x}\{[\frac{\sin 2\phi}{2}(HN_s\\&+(h+\overline{\eta}+\eta_{tr})N_b]\}+\frac{\partial}{\partial y}[H(S_s+\cos^2\phi\,N_s)+(h+\overline{\eta}+\eta_{tr})(S_b+\cos^2\phi\,N_b)]-\frac{\tau_{by}}{\rho}\end{aligned} \quad (9)$$

And the integral wave energy equation is

$$\begin{aligned}&\frac{1}{2}\frac{\partial}{\partial t}[\overline{\eta^2}+HW_s+(h+\overline{\eta}+\eta_{tr})W_b]+\frac{\partial}{\partial x}\{\cos\phi[H(F_s+K_s)+F_b(h+\overline{\eta}+\eta_{tr})]\}+\\&\cos^2\phi H\,N_s\frac{\partial U_s}{\partial x}+(N_b\cos^2\phi+\frac{W_b}{2})(h+\overline{\eta}+\eta_{tr})\frac{\partial U_b}{\partial x}+\frac{U_b}{2}\frac{\partial}{\partial x}[W_b(h+\overline{\eta}+\eta_{tr})]+\\&H\,N_s\frac{\sin 2\phi}{2}(\frac{\partial U_s}{\partial y}+\frac{\partial V_s}{\partial x})+(h+\overline{\eta}+\eta_{tr})N_b\frac{\sin 2\phi}{2}(\frac{\partial V_b}{\partial x}+\frac{\partial U_b}{\partial y})+\\&\frac{\partial}{\partial y}\{\sin\phi[H(F_s+K_s)+(h+\overline{\eta}+\eta_{tr})F_b]\}+(h+\overline{\eta}+\eta_{tr})(N_b\frac{\sin 2\phi}{2}+\frac{W_b}{2})\frac{\partial V_b}{\partial y}+\\&\frac{V_b}{2}\frac{\partial}{\partial y}[(h+\overline{\eta}+\eta_{tr})W_b]+HN_s\sin^2\phi\frac{\partial U_s}{\partial y}=-\frac{2}{3\pi}f_w\overline{U_b^{\,3}}-f_{wb}\,\omega\,H^2\end{aligned} \quad (10)$$

where H is the wave height, ϕ is the direction of wave propagation from the x-axis, f_w is the bottom friction factor and f_{wb} is a dimensionless factor for predicting energy dissipation rate due to wave breaking.

4. Simulation of Mean Wave Parameters in One Spatial Dimension

In a one-dimensional space with x denoting the direction of wave propagation, the integral continuity equation reads

$$\frac{\partial\overline{\eta}}{\partial t}+\frac{\partial}{\partial x}[H\,U_s+(h+\overline{\eta}+\eta_{tr})U_b]=0 \quad (11)$$

The dimensionless integral momentum equation becomes

$$\frac{\partial}{\partial t}[H U_s + (h+\bar{\eta}+\eta_{tr})U_b] + \frac{\partial}{\partial x}[H U_s^2 + (h+\bar{\eta}+\eta_{tr})U_b^2] = -(h+\bar{\eta})\frac{\partial \bar{\eta}}{\partial x} + \frac{\partial}{\partial x}[H S_s + (h+\bar{\eta}+\eta_{tr})S_b] - \frac{\tau_{bx}}{\rho} \tag{12}$$

and the dimensionless integral wave energy equation becomes

$$\begin{aligned}&\frac{1}{2}\frac{\partial}{\partial t}[Ep + H W_s + (h+\bar{\eta}+\eta_{tr})W_b] + \frac{\partial}{\partial x}[H F_s + (h+\bar{\eta}+\eta_{tr})F_b] \\ &= -\frac{\partial}{\partial x}(K_s H) - H N_s\frac{\partial U_s}{\partial x} - [(N_b + \frac{W_b}{2})(h+\bar{\eta}+\eta_{tr})]\frac{\partial U_b}{\partial x} \\ &\quad -\frac{U_b}{2}\frac{\partial}{\partial x}[W_b(h+\bar{\eta}+\eta_{tr})] - \frac{2}{3\pi}f_w\overline{U_b}^3 - f_{wb}\,\omega\, H^2\end{aligned} \tag{13}$$

4.1 Characteristic Equations and Numerical Solution

The integral equations (11)-(13) can be written into a quasilinear system

$$\frac{\partial \vec{q}}{\partial t} + A\cdot\frac{\partial \vec{q}}{\partial x} = S(x,t,\vec{q}) \tag{14}$$

where $\vec{q}$ is a dependent variable vector,

$$\vec{q} = \left[H, \bar{\eta}, U_b\right]^T \tag{15}$$

S is a source or sink vector, and A is a 3×3 Jacobian coefficient matrix. The propagation of the information described by Equation (14) can be characterized using the eigenvalues of the coefficient matrix, A. The eigenvalue of a matrix is defined as

$$\det[\lambda I - A] = 0 \tag{16}$$

where det denotes the determinant, λ is the eigenvalue, and I is a 3×3 unit matrix. Equation (16) is generally a third order polynomial in λ. If all three roots of the polynomial, λ_1, λ_2 and λ_3, are real and distinct, the system is hyperbolic. For a hyperbolic system, each eigenvalue denotes the propagation speed of some particular information. It is advantageous to obtain the numerical solutions of Equation (14) by the method of characteristics since the corresponding characteristic equations are ordinary differential equations.

The characteristic equations are established by combining the original system equations with an eigenvector of the coefficient matrix as follows

$$\vec{\ell}_i\cdot[\frac{\partial}{\partial t} + A\frac{\partial}{\partial x}]\vec{q} = \vec{\ell}_i\cdot S \qquad i = 1, 2, 3 \tag{17}$$

where $\vec{\ell}_i$ is the left eigenvector such that

$$\vec{\ell}_i\cdot[\lambda I - A] = 0 \tag{18}$$

Equation (17) can be written as ordinary differential equations

$$\vec{\ell}_i\cdot\frac{d\vec{q}}{dt} = \sum\vec{\ell}_i\cdot S \qquad i = 1, 2, 3 \tag{19}$$

along the characteristic curve

$$\frac{d}{dt} = \frac{\partial}{\partial t} + \lambda_i\cdot\frac{\partial}{\partial x} \tag{20}$$

The numerical solutions, say at a point “o” and at time level n, can be obtained by solving three characteristic equations integrated over the characteristic curves

$$\vec{\ell}_i \cdot (\vec{q}_o^{\,n} - \vec{q}_{x_j}^{\,n-1}) = \Delta t \cdot \Sigma \vec{\ell}_i \cdot S \qquad i, j=1,2,3 \tag{21}$$

where Δt is the time step, x_1, x_2 and x_3 denote three points traced back from the point "o" through three characteristic curves over one time step. Numerical stability requires that the Courant condition is satisfied

$$\frac{\Delta t \cdot |\lambda|_{max}}{\Delta x} \le 1 \tag{22}$$

where Δx is the spacing step and $|\lambda|_{max}$ is the maximum eigenvalue throughout the entire simulation period and over the entire computational domain.

To provide some insight into the characteristics of this system, eigenvalues and the corresponding eigenvectors are computed for three typical coastal conditions as shown in Table 1. T is the wave period, and L is the local wave length.

Table 1 Characteristics for Three Typical Coastal Conditions

Case	H (m)	T (sec)	h (m)	h/L	C_L (m/s)	C_g (m/s)	Eigenvalue (m/s)	Eigenvector ℓ_1	ℓ_2	ℓ_3
A	1.0	10	100	0.64	31.32	7.80	31.32	0.01	0.50	1.00
							8.32	1.00	-0. 01	-0.01
							-31.32	0.01	-0.50	1.00
B	1.0	10	10	0.11	9.90	8.02	10.00	0.28	1.00	0.61
							7.85	1.00	-0.19	-0.10
							-9.90	0.01	1.00	-0.61
C	1.0	10	2	0.04	4.43	4.45	5.24	0.63	1.00	0.23
							3.84	-0.61	1.00	0.29
							-4.48	0.01	1.00	-0.26

Cases A, B and C represent deep, intermediate and shallow water condition, respectively. The linear long wave speed $C_L=(gh)^{1/2}$ and wave group speed C_g estimated from Fourier approximation wave theory are included Table 1 for comparison with the eigenvalues. Based on the above investigation, the following observations are appropriate:

- In each of the three cases, the three eigenvalues are real and distinct. Thus the system is generally hyperbolic.
- In both Case A and Case B, the first and third eigenvalues are almost equal to the linear long-wave speed in magnitude. This is expected since the mean flow part of the system is similar to the shallow water wave equations, as stated in Section 2. The characteristics corresponding to these eigenvalues are termed wave characteristics(Katopodes and Strelkoff 1979).
- The second eigenvalue in each case is almost equal to the wave group speed. Thus the characteristics corresponding to this eigenvalue describes wave energy transfer, and they are accordingly termed energy characteristics(Xu 1996).
- As implied in Equation (17), the eigenvector measures the interaction among the characteristic equations. In Case A, the first component of the eigenvectors for the wave characteristics is always much smaller than the second and third components, while the first component of the eigenvector for the energy

characteristics is much greater than the other two components. This suggests that the wave energy transfer in deep waters is little affected by the mean flow circulation, and vice versa. From Case A to Case C, the first component ℓ_1 of the first eigenvector increases, suggesting that interaction between the mean flow and the wave energy transfer becomes stronger as the water shallows.

- In all three cases, the first component of the eigenvector of the third eigenvalue (negative) is always much smaller than other two components. This indicates that the backward propagation of the information described by the wave characteristics is little affected by the forward wave energy transfer.

4.2 Open Boundary Conditions

Numerical simulation in coastal engineering normally focuses on only a small portion of a larger system. Open boundaries are present at the locations of truncation from the larger system. In the numerical model, open boundary conditions must be specified to allow information to cross the open boundaries unhampered, as would be in the real situation.

For this case, three constraints are necessary and sufficient at the boundary. To permit interior information to propagate out of the domain, the characteristic equations corresponding to the eigenvalue denoting outgoing propagation should be used as part of the boundary conditions. In general, additional constraints would be required to supplement the characteristic equations for outgoing information. Ideally field data should meet such a need, but field data is only rarely available. Instead, additional (and artificial) conditions are generally called for. These extra boundary conditions coupled with the characteristic equations for outgoing information should be non-reflective or at most weakly reflective.

In this study, the Hedstrom(1979) approximate open boundary conditions are used whenever necessary. Hedstrom's approximate boundary conditions for a three-equation hyperbolic system are briefly described here. Suppose that of the three eigenvalues, m(<3) eigenvalues denote outgoing characteristics. The boundary conditions

$$\vec{\ell}_i \bullet \frac{\partial \vec{q}}{\partial t} = 0 \qquad (m < i \le 3) \tag{23}$$

prevents back reflection of waves into the solution domain from the boundary if there are only simple waves going out. In a linear case, the eigenvalues and eigenvectors are constant. The condition described by Equations (23) is equivalent to

$$\vec{\ell}_i \bullet \vec{q} = \text{ constant} \qquad (m < i \le 3) \tag{24}$$

This is the Riemann invariant along the incoming characteristics, i.e., the projection of the dependent variable vector on the incoming characteristic curve is constant.

Wave height is normally given at the offshore boundary as external forcing. Then only one of the Equation (23) conditions is needed, because the given wave height and the characteristic equation corresponding to outgoing waves would provide two boundary conditions. The extra condition corresponding to the wave characteristics should be used because the specification of wave height makes the condition corresponding to the energy characteristic redundant.

4.3 Application to Wave Propagation at Egmond Beach

The cross shore bottom profile at Egmond beach(Derks and Stive 1984) is shown in Figure 1. The incident wave period and height are 8.7 seconds and 2.46m, respectively. The wave forcing is suddenly imposed at the offshore boundary and persists throughout the simulation. The system is assumed to be initially quiescent, with wave height, wave setup and current all zero at the beginning of the simulation.

The computational domain is about 3000 m long, with a water depth at the offshore boundary of about 16 m. A uniform space step of 10 m is used with a corresponding time step of 0.7 second.

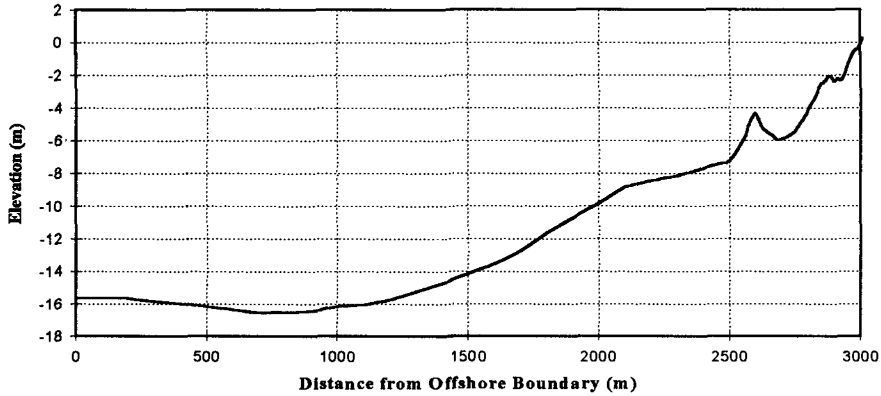

Figure 1 Bathymetric Profile At Egmond Beach

The wave height, wave setup and undertow velocity at eight time levels are shown in Figures 2 through 4. After seven minutes, a steady state wave height profile is established. It takes about fourteen minutes for the wave setup and undertow current to reach an equilibrium state. As waves approach to the shoreline, the mass transport is predominantly shoreward, causing a significant water surface pulse (Figure 3) and shoreward mass transport. After waves reach the shoreline, seaward undertow current develops(Figure 4). The transient wave setup and undertow current are much greater than steady state wave setup and undertow current, suggesting that the transient dynamics in coastal process could be very important. The observed (Derks and Stive 1984) wave height and setup are also plotted in Figures 2 and 3 as the small circles. Good agreement is found for both wave height and wave setup.

The above case study leads to the following conclusions: (1) the numerical scheme is appropriate for simulating the evolution of mean wave parameters in one spatial dimension; (2) the open boundary conditions work satisfactorily.

5. Simulation of Mean Wave Parameters in Two Spatial Dimensions

The integral governing equations in two spatial dimensions, Equations (7) through (10), can be written in the quasilinear form

$$\frac{\partial \vec{q}}{\partial t} + A_x \frac{\partial \vec{q}}{\partial x} + A_y \frac{\partial \vec{q}}{\partial y} = S \tag{25}$$

where $\vec{q}$ is the dependent variable vector, $\vec{q} = [H, \overline{\eta}, U_b, V_b]$, A_x and A_y are the

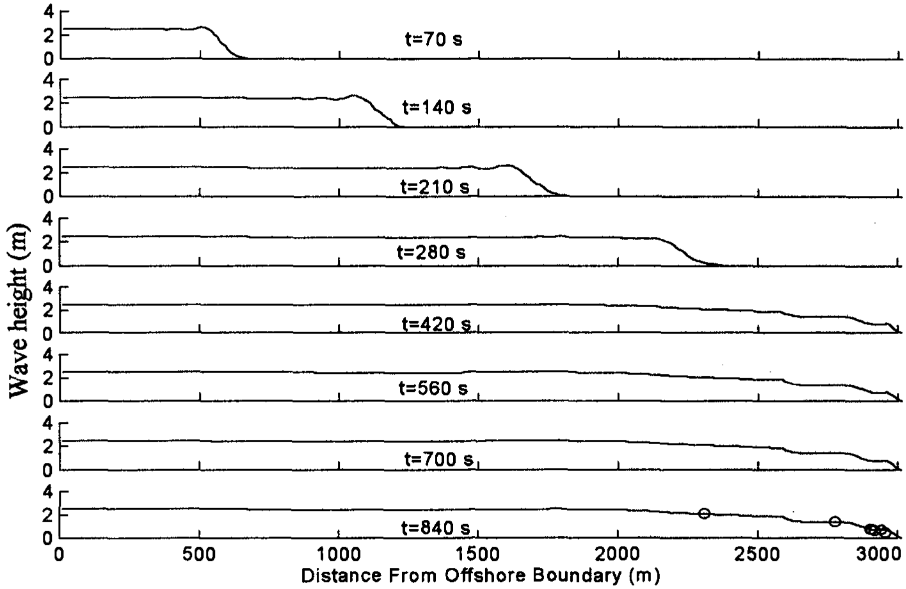

Figure 2 Evolution of Wave Height Profile

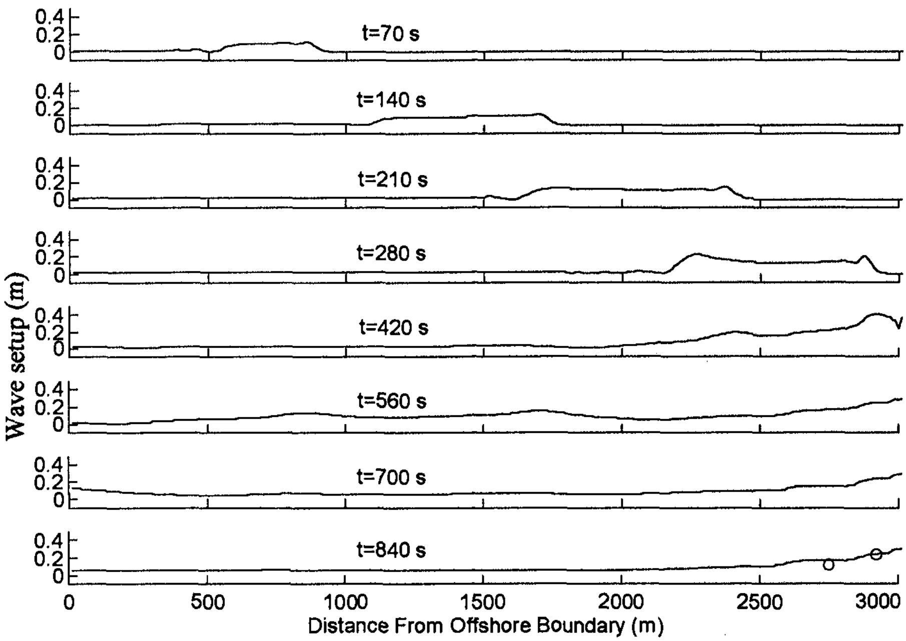

Figure 3 Evolution of Mean Water Surfaces

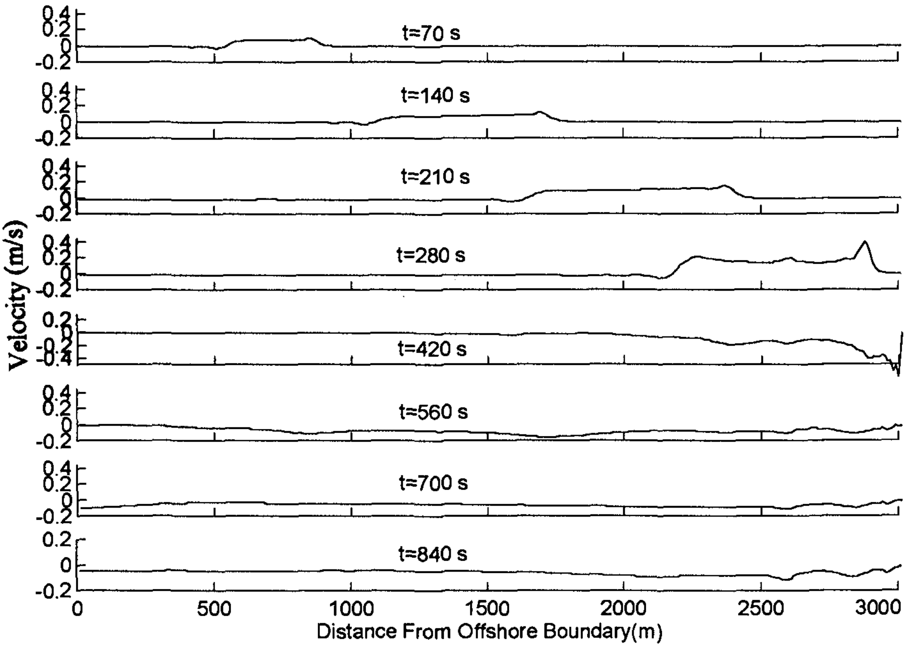

Figure 4 Evolution of Undertow Velocity

coefficient matrices, and S denotes the sink or source vector. Due to the limit of space for this paper, the complexity of the integral equations and, the introduction of closure variables, the exact expressions for the coefficient matrices and the sink terms are not presented here; see Xu (1996) for details.

5.1 Characteristic Equations and System Properties

Again the information propagation described by equation (25) can be characterized using the eigenvalues of the coefficient matrices, A_x and A_y. In two spatial dimensions, however, the eigenvalues are azimuth-dependent. If the azimuth on the x-y plane is denoted by a normal vector $\vec{n}\,[\cos(\theta), \sin(\theta)]$, then the eigenvalues for Equation (25) are defined as

$$\det[\lambda \cdot I - A_x \cos(\theta) - A_y \sin(\theta)] = 0 \tag{26}$$

which in general is a fourth order polynomial in λ. If the four roots of λ are all real and distinct, the system is hyperbolic. The eigenvalues for the entire range of the azimuth form a family of characteristic surfaces with its normal vector defined as $[-\lambda, \cos(\theta), \sin(\theta)]$. These characteristic surfaces are generally inscribed by a cone. The generation lines of the cone are termed bi-characteristics. The characteristic equations can be derived by linearly combining the system equations through the eigenvector of the coefficient matrices

$$\vec{\ell}_j\left(\frac{\partial \vec{q}}{\partial t} + A_x \frac{\partial \vec{q}}{\partial x} + A_y \frac{\partial \vec{q}}{\partial y}\right) = \vec{\ell}_j S \qquad j = 1..4 \tag{27}$$

where $\vec{\ell}_j$ is the left eigenvector

$$\vec{\ell}_i\left[\lambda \cdot I - A_x \cos(\theta) - A_y \sin(\theta)\right] = 0 \tag{28}$$

On the characteristic surfaces, the characteristic equations can be written with differentiations in two directions only, conventionally along the bi-characteristics and a cross-direction which is almost perpendicular to the bi-characteristics. Such characteristic equations are still partial differential equations. There are infinite sets of eigenvalues and characteristic equations at a point since they are azimuth-dependent.

To appreciate the characteristics of this system, the eigenvalues are computed numerically for the following condition: wave direction $\phi=\pi/2$, wave height=1.0 m, water depth h=10 m, mean water elevation $\overline{\eta}=0$, and mean flow velocities under wave trough U_b=0.5 m/s and V_b=0.5 m/s. The eigenvalues as a function of the azimuth in the range from 0 to 2π are shown in Figure 5. Also shown in the figure are the three eigenvalues of the shallow water wave equations under the same condition along with their analytical expressions. Of the four eigenvalues at each azimuth, two are identified by λ_w, denoting wave characteristics, one labeled by λ_e, referring to the energy characteristic, and the fourth by λ_f denoting the flow characteristic(Katopodes 1979). The flow characteristics is an extra characteristic family in the two spatial dimensions. The magnitude of the eigenvalue of the flow characteristics is the same order of the magnitude as the flow velocity. The following observations are appropriate:

- This system is generally hyperbolic because the four eigenvalues at any azimuth under the given condition are real and distinct.
- Under the assumed condition, the eigenvalues of wave and flow characteristics are almost identical to those for the shallow water wave equations. The eigenvalue of the energy characteristics may be approximated by $C_g \cos(\phi - \theta)$, in which C_g is the plane wave group speed.

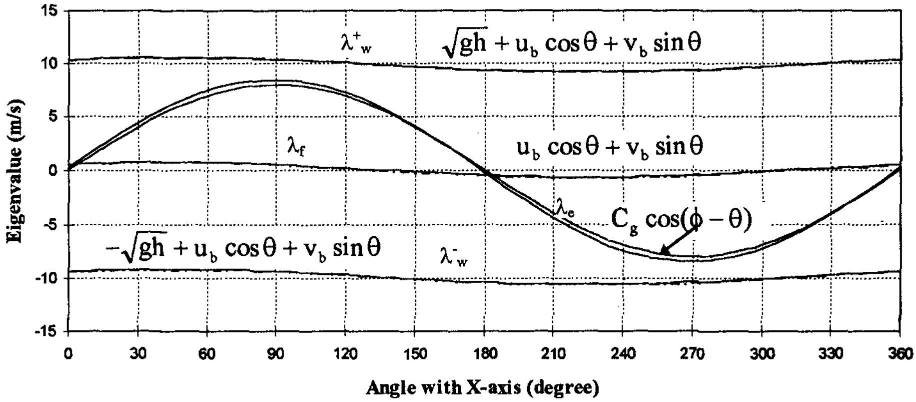

Figure 5 Variation Of Eigenvalue λ With Azimuth θ

- The eigenvalues λ_w^+ and λ_w^- of the wave characteristics are identical when considering the entire range of azimuth (0, 2π) since $\lambda_w^+(\theta)=-\lambda_w^-(\theta+\pi)$. Only one of them, conventionally λ_w^+, is used in describing wave characteristics. The eigenvalues of the wave characteristics vary slightly with azimuth. Information spreads out at an almost uniform speed.
- The maximum eigenvalue is of particular importance to numerical simulation because it defines the domain of influence or dependence. The direction corresponding to the maximum eigenvalue is termed a principal direction (Xu 1996). In the principal direction, the eigenvalues and characteristic equations of the shallow water wave equations in two spatial dimensions are the same as those in one spatial dimension

5.2 Numerical Scheme

The method of characteristics is used to obtain numerical solutions. The major issues in numerically simulating the evolution of mean wave parameters in two spatial dimensions are (1) evaluation of wave propagation direction, which is used in the closure of wave apparent stresses, (2) development of a numerical scheme recognizing that there are infinite characteristic equations, (3) open boundary conditions, and (4) evaluation of derivatives in the cross direction (cross-derivatives). Due to the limit of space here, the evaluation of wave direction is not discussed.

The bi-characteristic method proposed by Bulter (1962) is adapted to develop a numerical scheme for the present system. This method is based on the combination of the characteristic equations along several bi-characteristics to minimize the coefficients of the cross derivatives. A total of six directions are involved in this case.

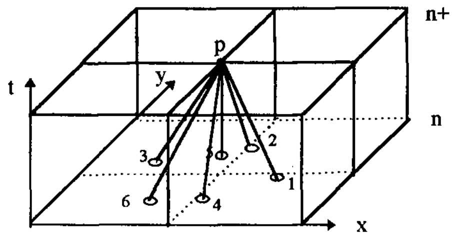

Figure 6 Illustration of Bi-characteristics Scheme

The six points traced back from point "p" by the respective characteristic velocity are labeled as 1 to 6 at time level n. Of the six points, 1,2,3 and 4 are on the wave bi-characteristics corresponding to azimuth θ=0, π/2, π and 3π/2, respectively. Point 5 is on the flow path, and point 6 is along the wave propagation direction. The coordinates of the points 1 through 6 can be estimated by using the following expressions with sufficient accuracy (Xu 1996)

$$\begin{aligned} x_{2,4,5} &= x_p - U_b\Delta t; \quad & x_{1,3} &= x_p - (U_b \mp C)\Delta t; \quad & x_6 &= x_p - \lambda_e \Delta t \cos\phi \\ y_{2,4,5} &= y_p - V_b\Delta t; \quad & y_{1,3} &= y_p - (V_b \mp C)\Delta t; \quad & y_6 &= y_p - \lambda_e \Delta t \sin\phi \end{aligned} \tag{29}$$

where C is the long wave speed and ϕ is the wave propagation direction. The values at these points are interpolated from the values at surrounding grid points.

The integration of the energy characteristic equation along 6-p gives

$$\ell_1^6 H_p + \ell_2^6 \overline{\eta}_p + \ell_3^6 U_{b,p} + \ell_4^6 V_{b,p} = \ell_1^6 H_6 + \ell_2^6 \overline{\eta}_6 + \ell_3^6 U_{b,6} + \ell_4^6 V_{b,6} + [a_6 \frac{\partial H}{\partial x} + b_6 \frac{\partial H}{\partial y} + c_6 \frac{\partial \overline{\eta}}{\partial x} + d_6 \frac{\partial \overline{\eta}}{\partial y} + e_6 \frac{\partial U_b}{\partial x} + f_6 \frac{\partial U_b}{\partial y} + g_6 \frac{\partial V_b}{\partial x} + h_6 \frac{\partial V_b}{\partial y} + S_6] \cdot \Delta t \tag{30}$$

Summing up the four wave characteristic equations along 1-p, 2-p, 3-p and 4-p and subtracting twice the continuity equation along 5-p gives

$$\begin{aligned}
&(\sum_{i=1,4} \ell_1^i) H_p + (\sum_{i=1,4} \ell_2^i - 2)\overline{\eta}_p + (\sum_{i=1,4} \ell_3^i) U_{b,p} + (\sum_{i=1,4} \ell_4^i) V_{b,p} = \\
&[\sum_{i=1,4} \ell_1^i H_i + (\sum_{i=1,4} \ell_2^i \overline{\eta}_i - 2\overline{\eta}_5) + \sum_{i=1,4} \ell_3^i U_{b,i} + \sum_{i=1,4} \ell_4^i V_{b,i} + \\
&(\sum_{i=1,4} a_i)\frac{\partial H}{\partial x} + (\sum_{i=1,4} b_i)\frac{\partial H}{\partial y} + (\sum_{i=1,4} c_i)\frac{\partial \overline{\eta}}{\partial x} + (\sum_{i=1,4} d_i)\frac{\partial \overline{\eta}}{\partial y} + \\
&(\sum_{i=1,4} e_i)\frac{\partial U_b}{\partial x} + (\sum_{i=1,4} f_i)\frac{\partial U_b}{\partial y} + (\sum_{i=1,4} g_i)\frac{\partial V_b}{\partial x} + (\sum_{i=1,4} h_i)\frac{\partial V_b}{\partial y} + (\sum_{i=1,4} S_i)] \cdot \Delta t
\end{aligned} \tag{31}$$

Subtracting the wave characteristic equation along 1-p from that along 3-p gives

$$\begin{aligned}
&(\ell_1^1 - \ell_1^3)H_p + (\ell_2^1 - \ell_2^3)\overline{\eta}_p + (\ell_3^1 - \ell_3^3)U_{b,p} + (\ell_4^1 - \ell_4^3)V_{b,p} = \\
&\ell_1^1 H_1 - \ell_1^3 H_3 + \ell_2^1 \overline{\eta}_1 - \ell_2^3 \overline{\eta}_3 + \ell_3^1 U_{b,1} - \ell_3^3 U_{b,3} + \ell_4^1 V_{b,1} - \ell_4^3 V_{b,3} + \\
&[(a_1 - a_3)\frac{\partial H}{\partial x} + (b_1 - b_3)\frac{\partial H}{\partial y} + (c_1 - c_3)\frac{\partial \overline{\eta}}{\partial x} + (d_1 - d_3)\frac{\partial \overline{\eta}}{\partial y} + (e_1 - e_3)\frac{\partial U_b}{\partial x} \\
&+ (f_1 - f_3)\frac{\partial U_b}{\partial y} + (g_1 - g_3)\frac{\partial V_b}{\partial x} + (h_1 - h_3)\frac{\partial V_b}{\partial y} + S_1 - S_3] \cdot \Delta t
\end{aligned} \tag{32}$$

Similarly, subtracting the characteristic equation along 2-p from that along 4-p gives

$$\begin{aligned}
&(\ell_1^2 - \ell_1^4)H_p + (\ell_2^2 - \ell_2^4)\overline{\eta}_p + (\ell_3^2 - \ell_3^4)U_{b,p} + (\ell_4^2 - \ell_4^4)V_{b,p} = \\
&\ell_1^2 H_2 - \ell_1^4 H_4 + \ell_2^2 \overline{\eta}_2 - \ell_2^4 \overline{\eta}_4 + \ell_3^2 U_{b,2} - \ell_3^4 U_{b,4} + \ell_4^2 V_{b,2} - \ell_4^4 V_{b,4} + \\
&[(a_2 - a_4)\frac{\partial H}{\partial x} + (b_2 - b_4)\frac{\partial H}{\partial y} + (c_2 - c_4)\frac{\partial \overline{\eta}}{\partial x} + (d_2 - d_4)\frac{\partial \overline{\eta}}{\partial y} + (e_2 - e_4)\frac{\partial U_b}{\partial x} \\
&+ (f_2 - f_4)\frac{\partial U_b}{\partial y} + (g_2 - g_4)\frac{\partial V_b}{\partial x} + (h_2 - h_4)\frac{\partial V_b}{\partial y} + S_2 - S_4]\Delta t
\end{aligned} \tag{33}$$

It can be verified that the coefficients of the cross derivatives through these combinations are much smaller than those without using such combinations. Equations (30) through (33) are used to obtain the solutions for H, $\overline{\eta}$, U_b and V_b.

5.3 Open Boundary Conditions

At an open boundary, some bi-characteristics lie outside the computational domain. So only some of Equations (30) through (33) can be derived. As a result, extra boundary conditions need to be specified.

In the study of the characteristics of the shallow water wave equations, it is found that the characteristics along a flow path in a two dimensional space behave exactly the same as in a one-dimensional space(Xu 1996). Heuristically, the Hedstrom open boundary conditions introduced in Section 4.2 may be extended approximately to two spatial dimensional problems as long as the open boundary conditions are applied in the flow direction.

If there are m outgoing characteristics, then the 4-m Hedstrom approximate boundary conditions in the flow direction are formed as

$$\vec{\lambda}_j \bullet \frac{\partial \vec{q}}{\partial t} = 0 \qquad j = m..4 \tag{34}$$

5.4 Simulation of Oblique Wave Propagation

To test the performance of the numerical scheme and open boundary conditions, the numerical model is applied to simulate oblique wave propagation. Waves are assumed to propagate into an initially quiescent square domain from the left lower corner at an angle of 45° with the x-axis. The water depth of the domain is 10 m, and the incident wave height is 0.5 m with a wave period of 10 seconds. A uniform grid with $\Delta x = \Delta y = 10$m is used, coupled with a time step of 0.5 second. Wave height is gradually imposed at the inflow boundaries over three time steps.

The computed wave height surfaces at six time levels are shown in Figure (7). At time 50 seconds, waves pass through the computational domain, and a steady state wave field is established. The solutions at the inflow and outflow boundaries are smooth at all six time levels, demonstrating that the imposed boundary conditions do not cause any appreciable numerical reflection at the boundaries.

The propagation speed is estimated by dividing the distance by the time interval. The estimated speed of energy transfer is 8.25 m/s, which is close to the wave group speed estimated from Fourier approximation wave theory of 8.34 m/s.

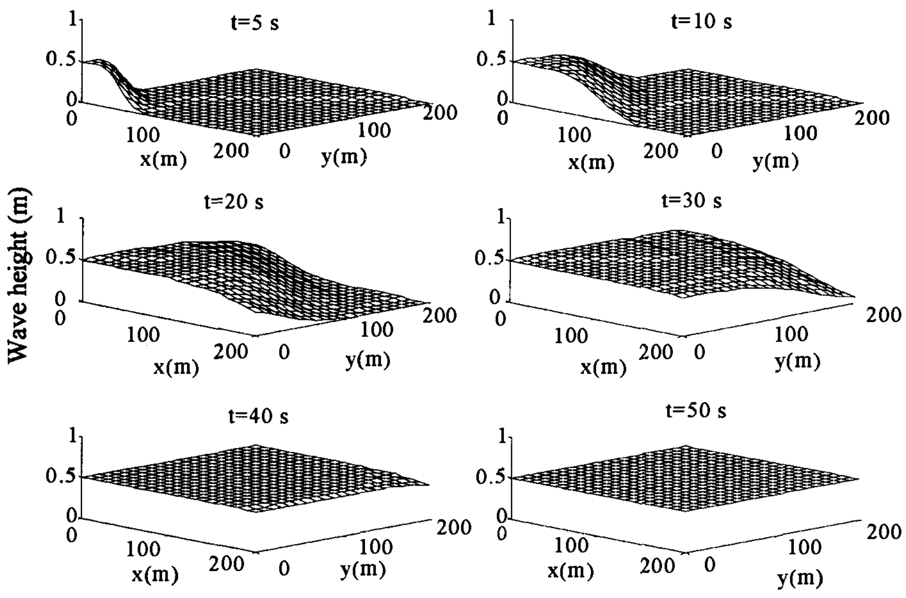

Figure 7 Evolution of Wave Height Envelops

6. Summary

In this study, a wave-averaged depth-integrated model for the evolution of mean wave parameters was developed. This model is valid for both shoaling waves and surf zones provided that periodic motion is dominant over turbulence. The physical processes that this model can simulate include wave shoaling, refraction, diffraction, wave-current interaction and mean flow circulation, etc. The proposed numerical scheme can be used to obtain the numerical solutions effectively and with negligible reflection at open boundaries. The transient behavior in the evolution of mean wave field can be adequately modeled.

It was clearly shown in this study that transient dynamics may be important for coastal evolution. The wave-driven current and mean water surface variation are significantly greater than the respective steady state values. Since the wave conditions in deep water are rarely invariant, the simulation of transient behavior is a significant feature of this model.

References

Bulter, D.S., 1960. *The Numerical Solution of Hyperbolic Systems of Partial Differential Equations in Three Independent Variables*. Proc. Royal Soc.(London), 255A, pp.232-252

Derks, H. and Stive, M.J.F., 1984. *Field Investigation in the TOW Study Programme for Coastal Sediment Transport in the Netherlands:* . Proc. 19th Conf. Coastal Eng., Houston, Volume II, Chapter 123, pp. 1830-1845.

Hedstrom, G.W., 1979. *Non-reflecting Boundary Conditions for Nonlinear Hyperbolic Systems*. Computational Physics, Vol.30, pp.222-237.

Katopodes, N. and Strelkoff, T., 1979. *Two Dimensional Shallow Water-Wave Models*. Journal of Engineering Mechanics, Vol.105, No. EM2. pp. 317-334.

Sobey, R.J. and Thieke, R.J., 1989. *Mean Flow Circulation Equations For Shoaling And Breaking Waves*. Journal of Engineering Mechanics. 115: 285-303.

Xu, Jianlu. 1996. *A Time-Averaged Approach to Wave Evolution from Deep Water to Shallow Water*. Ph.D. Thesis, University of California at Berkeley [Available from University Microfilms].